Development of Transparent Acellular Dermal Matrix as Tissue-Engineered Stroma Substitute for Central Lamellar Keratoplasty

Yuexin Wang, Jiahui Ma, Xiaodan Jiang, Ziyuan Liu, Jiarui Yang, and Xuemin Li

Department of Ophthalmology, Peking University Third Hospital, Beijing, China

PURPOSE. To improve the transparency of the acellular dermal matrix (ADM) and investigate the optical, mechanical and histologic properties and biocompatibility of transparent ADM (TADM) in lamellar keratoplasty.

METHODS. A stepwise sectioning strategy was applied to determine the transparency distribution of the ADM, and TADM was fabricated accordingly. Transmittance measurements, uniaxial tension testing, and histologic staining were applied to detect its properties. Lamellar keratoplasty was performed in rabbits with TADM, and postoperative evaluations were conducted including the transmittance of the transplant area and histologic staining.

RESULTS. The transmittance of the ADM increased with increasing depth, and TADM was isolated mechanically at the deepest level. There was a significant improvement in the transmittance of the TADM compared with the ADM, and no significant difference in transmittance between dehydrated TADM and cornea was observed. The elastic modulus of TADM was significantly stronger than that of normal cornea ($P = 0.004$). TADM consisted of dense collagen fibrils, mainly collagen type I, and the collagen fibril diameter and interfibrillar spacing were determined to be larger than corneal stroma. After lamellar keratoplasty in rabbits, the TADM was well integrated with the host cornea, and transparent cornea without neovascularization was observed at 6 months. Re-epithelization was completed at 1 month, and keratocyte repopulation and collagen remodeling were observed in the graft 3 and 6 months after surgery.

CONCLUSIONS. This study presents the transparency distribution of the ADM and a method for obtaining TADM, which demonstrates ideal transparency, strong mechanical properties, and satisfactory biocompatibility when applied in lamellar keratoplasty.

Keywords: lamellar keratoplasty, acellular dermal matrix, corneal substitute, tissue engineering

Corneal diseases are one of the leading causes of blindness caused by irreversible damage to the optical quality of the cornea.[1] Cornea transplantation with donor grafts is the most widely accepted treatment for restoring corneal blindness.[2] However, a severe global donor cornea shortage is the leading limitation, especially in developing countries.[3] In addition to this shortage, postoperative rejection and inflammation are obstacles for successful procedures.[4]

This demand is promoting the development of bioengineered cornea substitutes. The stroma accounts for more than 90% of the cornea; furthermore, lamellar keratoplasty, which replaces the stroma layer of the cornea, demonstrates a significant advantage over penetrating keratoplasty.[5] Thus various studies have targeted the replacement of the stroma with biomaterials and have made significant progress. Current investigations consist of collagen-, stroma-, and cell-based approaches to construct stroma substitutes, and many studies have tested the substitute in vivo for corneal regeneration.[6,7] However, very few products have been tested in clinical trials or applied in clinical practice.[4]

In deriving the acellular dermal matrix (ADM) from donor dermis, the collagen scaffold is retained, while the cellular components are removed; the resulting material can support tissue regeneration and native cell ingrowth after transplantation.[8] Our previous research demonstrated that the ADM had a structure similar to that of the corneal stroma and supported keratocyte repopulation by 24 weeks after marginal corneal intrastromal keratoplasty in rabbits.[9] Additionally, our clinical trial demonstrated ideal biocompatibility and safety when applying the ADM in intrastromal lamellar keratoplasty for patients with pellucid marginal corneal degeneration.[10] However, the transparency of the applied ADM needed to be improved before it could be used in central lamellar keratoplasty. Theoretically, the histologic structures of the human dermis vary with depth. Thus the transparency of the ADM could also vary with depth.

This study aimed to identify the transparency distribution of the ADM with depth, obtained transparent acellular dermal matrix (TADM) accordingly, and further examined its properties in vitro and in vivo to demonstrate its

biocompatibility and its feasibility for application in lamellar keratoplasty.

MATERIALS AND METHODS

Materials and Animals

Commercially available ADM (Qingyuan Weiye Bio-tissue Engineering, China) was used and was referred to as *the original ADM*. New Zealand white rabbits (Center for Experimental Animals of Peking University Health Science Center, Beijing, China) were obtained. The present research complied with the Animal Research: Reporting In Vivo Experiments (ARRIVE) guidelines, and the animals were handled in accordance with the Association for Research in Vision and Ophthalmology. The research protocol was approval by the local review board.

Transparency Distribution Examination and Improved Transparency ADM Fabrication

The original ADM (n = 5), approximately 6 mm in diameter, was immersed in 20% sucrose solution at 4° C for 24 hours. Then, the sample was embedded in Optical Coherence Tomography (OCT) media (Sakura Finetek, Torrance, CA) oriented with the plane perpendicular to the lid. After being frozen, the sample was fixed onto the platform of a cryostat (CM1950, Leica, Germany) with the plane parallel to the blade. Cryosectioning was performed with the thickness set at 50 μm. Each sectioned lamella was transferred to a well prefilled with 100 mL of phosphate-buffered saline solution (PBS) in a 96-well plate, and each lamella was carefully flattened at the bottom of the well. Wells with PBS alone were used as controls. The absorbance at wavelengths of 490 nm, 570 nm, and 630 nm was measured with a spectrophotometer (BioTek, Winooski, VT) and converted to transmittance accordingly. After identifying the location of the most transparent layer, the matrix surrounding the most transparent layer was isolated from the full-thickness ADM stored in PBS using an electric dermatome (Zhili Medical, Shanghai, China) preset to the target thickness according to the experimental requirements. The isolated matrix was regarded as TADM and was stored in glycerol for dehydration.

Histological Staining

For ADM, a 5 × 5 mm ADM rectangle (n = 3) was sampled. Cryosectioning was conducted parallel to the surface at a thickness of 7 μm. During the sectioning process, 10 consecutive specimens were sampled every 60 sections. Three groups of specimens were obtained and considered superficial, intermediate and deep layers of the ADM. For TADM and the postoperative cornea, a 5 × 5 mm TADM rectangle (n = 3) of approximately 500 μm and cornea of the transplant area 3 (n = 4) and 6 (n = 4) months after transplantation were sampled. Sectioning was performed vertical to the surface.

Standard hematoxylin and eosin (H&E) and picrosirius red staining were performed on the original ADM, TADM, and posttransplantation cornea. The sections of posttransplantation cornea were additionally stained with cytokeratin 3/12 (Abcam, Cambridge, UK) and CD68 (Abcam) by standard immunohistochemical procedures. The H&E and immunochemical staining results were observed and imaged using a NanoZoomer (Hamamatsu Phototonics, Hamamatsu, Japan). The picrosirius red staining results were observed and imaged using a polarizing microscope (DM2500; Leica, Wetzlar, Germany). Picrosirius red dye can enhance the birefringence of collagen, facilitating the identification of type I and III collagen based on the color when exposed to polarized light.[11]

Electron Microscopy

TADM samples (n = 3) of approximately 1 × 1 cm in size and 500 μm thickness were prepared for transmission electron microscopy (TEM). The specimens were sectioned vertical to their surface, treated according to routine procedures and observed with a transmission electron microscope (JEM-1400; JEOL, Tokyo, Japan). Quantitative analysis of the collagen fibril diameter and interfibrillar spacing was performed with Fuji software (National Institutes of Health, Bethesda, MD). For the diameter, the circular spots of collagen fibrils on the TEM image were separated, and their diameters were measured. The interfibrillar space was calculated according to a formula described previously.[12]

Lamellar Keratoplasty

Rabbits (n = 8) were generally anesthetized with 25 mg/kg sodium pentobarbital (Merck, Darmstadt, Germany) and topically anesthetized with 0.4% oxybuprocaine hydrochloride (Benoxil; Santen Pharmaceutical, Osaka, Japan). The right eye remained unoperated, and the surgery was performed on only the left eye of all rabbits. The cornea of the left eye was marked with a 6-mm stainless trephine, and the stroma was excised at depths of three-fourths of the full thickness with a crescent knife (Alcon, Fort Worth, TX). TADM of approximately 300 μm was hydrated for 10 minutes in PBS before being tailored with the same 6-mm trephine. The tailored TADM disk was transplanted onto the recipient cornea bed and immobilized with 12 interrupted 10-0 nylon sutures. After surgery, 0.5% levofloxacin drops (Santen Pharmaceutical, Osaka, Japan) and 1% prednisolone acetate ophthalmic suspension (Pred Forte; Allergan, Dublin, Ireland) were applied three times a day for 2 weeks. The sutures were removed on significant loosening.

Postoperative Observation

The postoperative clinical evaluation consisted of the observation of ocular and graft signs were conducted 1 week, 1 month, 3 months, and 6 months after surgery using an IM 900 slit lamp microscope (Imaging module 900; Köniz, Bern, Switzerland). Re-epithelization was evaluated by fluorescein staining observed under cobalt-blue light. The thickness of the central cornea and edema of the transplantation area were assessed by anterior segment optical coherence tomography (AS-OCT, Zeiss, Germany) 1 month, 3 months, and 6 months after surgery.

At 3 and 6 months after surgery, half of the rabbits (n = 4) chosen randomly were killed with an overdose of anesthesia, and the transplant area was entirely excised with a 6-mm trephine for evaluation of its transparency and histology.

Transparency Examination

A 6-mm trephine was used to sample ADM, TADM of approximately 500 μm preserved in glycerol, normal cornea
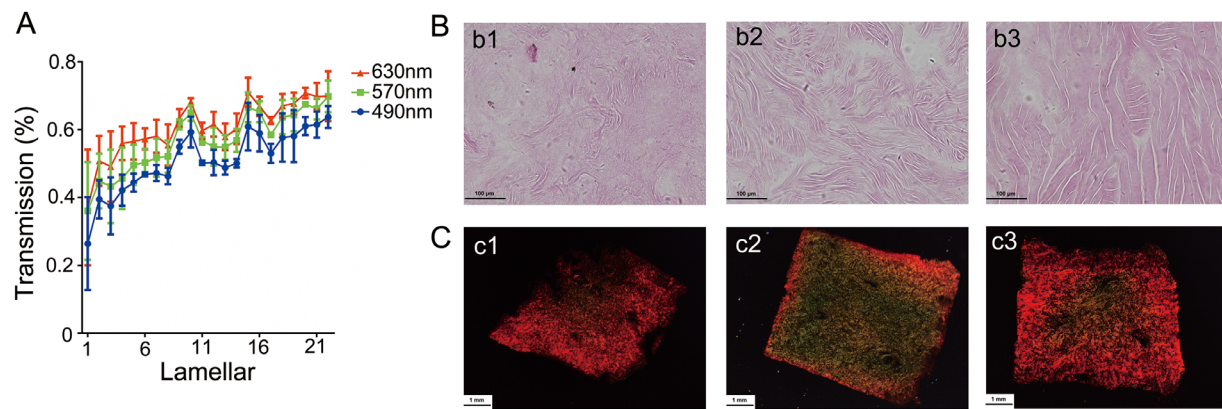
FIGURE 1. Transparency and histology distribution. Light transmission, H&E staining and picrosirius red staining of different ADM lamellae. **(A)** Light transmission of different lamellae with increasing depth (n = 5). **(B)** H&E staining of the superficial ADM layer *(b1)*, intermediate ADM layer *(b2)*, and deep ADM layer *(b3)*. **(C)** Picrosirius red staining of the superficial ADM layer *(c1)*, intermediate ADM layer *(c2)*, and deep ADM layer *(c3)* (representative of 3 independent experiments).

and the transplant area 3 months and 6 months after surgery. After sampling, hydrated TADM in this experiment was prepared after immersion in PBS for 10 min. ADM, dehydrated TADM, hydrated TADM and full-thickness cornea were photographed with a background of the word "CORNEA" for gross observation. For quantitative examination, the thickness of ADM, dehydrated TADM, hydrated TADM and full-thickness cornea were measured by a thickness gauge (accuracy of 0.01 mm, Wujin, China). ADM, dehydrated TADM (n = 5) was transferred to a 96-well plate prefilled with 100 µL of glycerol. Hydrated TADM hydrated in PBS for 10 minutes (n = 5) and normal cornea (n = 5) were transferred to wells prefilled with 100 µL of PBS. Glycerol and PBS without specimens were treated as controls. The absorbance from 350–900 nm at 10-nm intervals was examined using a spectrophotometer (BioTek). The absorbance of dehydrated and hydrated TADM was adjusted according to their thickness relative to that of the normal cornea. The transmittance was calculated according to the absorbance.

Mechanical Properties Testing

Uniaxial tension testing was applied using a material testing machine (EZ-LX; Shimadzu, Kyoto, Japan) to evaluate the mechanical properties of the dehydrated TADM (n = 5), hydrated TADM (n = 5), and rabbit cornea (n = 5). Cornea with 3 mm of sclera was obtained from unoperated rabbits and tailored into symmetrical strips with wide ends and a narrow waist (3 mm). TADM samples of approximately 500 µm in thickness were cut into a similar shape with an approximately 3-mm waist and 15 mm in length. A thickness gauge (accuracy of 0.01 mm) was used to measure the thickness (t). The width (w) and the initial distance (L0) between the clamps were measured by a Vernier caliper. The uniaxial tension test was conducted at a velocity of 2 mm/min; the sampling frequency was 10 Hz. The original load-displacement (F-△L) data were recorded. Stress (σ) was calculated under each load as F/wt. The strain (ε) was obtained by calculating △L/L0. Origin 8.0 software was applied to create and analyze the stress-strain curve. The tangent modulus (E_t) was calculated by taking the first derivative of the stress-strain curve ($E_t = d\sigma/d\varepsilon$). The E_t at stresses of 10 and 100 KPa was recorded. The linear segment of the stress-strain curve was linearly fitted, and the slope was obtained as the elastic modulus.

Data Analysis

SPSS software (version 23.0) was applied for statistical analysis. The data are presented as the mean ± SD. The unpaired Student's *t*-test was performed for comparisons between two groups, and one-way analysis of variance with Bonferroni's post hoc test was performed for comparisons of multiple groups. $P < 0.05$ was considered to represent a significant difference.

RESULTS

ADM Transparency and Histological Distribution and TADM Fabrication

As shown in Figure 1A, the light transmittance gradually increased as the lamellar number increased, which indicated increasing depth at 490, 570, and 630 nm ($P < 0.001$, $P < 0.001$, $P < 0.001$, respectively). H&E staining demonstrated that collagen bundles became significantly thicker and more organized as the depth increased, as shown in Figure 1B. Picrosirius red staining of the different lamella, as shown in Figure 1C, revealed that the superficial layers mainly consisted of collagen type I, the intermediate layers comprised a large amount of collagen type III, and the deep layers contained mostly collagen type I with a small amount of collagen type III.

According to the transparency distribution, histology and collagen composition of the original ADM, the deeper layers were more transparent and uniform in structure than the superficial layers. Thus the deepest ADM lamellae of various thicknesses according to experimental requirements were mechanically isolated using an electric dermatome for application as TADM.

TADM Transparency

As shown in Figure 2A, the dehydrated TADM exhibited ideal transparency, similar to that of normal cornea, on gross examination. The transmittance of dehydrated and hydrated TADM was significantly better than that of ADM at
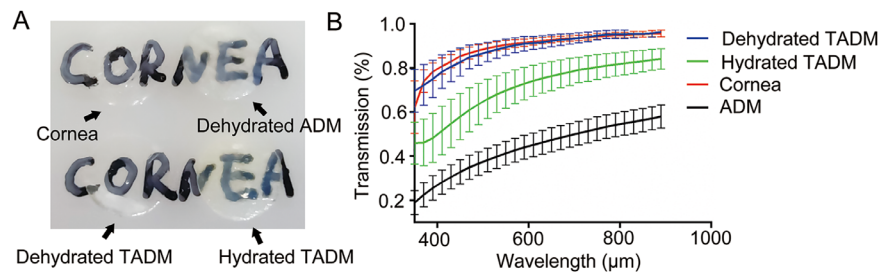
Figure 2. Transparency of TADM. Transparency of TADM on gross observation and light transmittance examination. **(A)** Gross observation of dehydrated and hydrated TADM compared with cornea. **(B)** Light transmittance of dehydrated and hydrated TADM compared with cornea (n = 5).
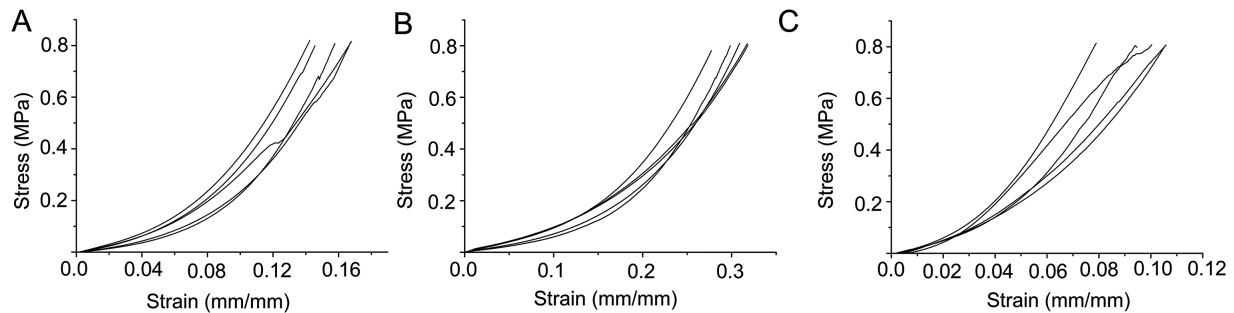
Figure 3. Mechanical properties of TADM. Stress-stain curves of dehydrated and hydrated TADM and cornea. **(A)** Stress-stain curve of dehydrated TADM (n = 5). **(B)** Stress-stain curve of hydrated TADM (n = 5). **(C)** Stress-stain curve of cornea (n = 5).

Table. Parameters of Uniaxial Tension Test for Dehydrated and Hydrated TADM and Cornea

	Tangent modulus (MPa)		
	10 KPa	**100 KPa**	**Elastic modulus (MPa)**
Dehydrated TADM (n = 5) (Mean ± SD)	1.29 ± 0.39	3.08 ± 0.35	25.3 ± 1.54
Hydrated TADM (n = 5) (Mean ± SD)	0.75 ± 3.25	1.54 ± 0.95	6.35 ± 1.39
Cornea (n = 4) (Mean ± SD)	2.70 ± 0.39	5.72 ± 1.25	17.23 ± 4.24
P value			
Dehydrated TADM versus cornea	<0.001	<0.001	0.004
Hydrated TADM versus cornea	<0.001	<0.001	<0.001
Dehydrated versus hydrated TADM	0.118	0.021	<0.001

TADM: transparent acellular dermal matrix

any wavelength from 350–900 nm, as shown in Figure 2B ($P < 0.05$). There were no differences in transmittance between the dehydrated TADM and normal cornea ($P > 0.05$). The TADM showed a significant decrease in transmission after hydration in PBS for 10 minutes ($P < 0.05$).

Mechanical Properties of the TADM

Similar to the rabbit cornea, the dehydrated and hydrated TADM exhibited a typical stress-strain curve for viscoelastic materials, as shown in Figures 3A and 3B. The tangent moduli of the dehydrated TADM at stresses of 10 and 100 KPa were significantly lower than those of the control cornea ($P < 0.001$, respectively), as shown in the Table. A significantly higher elastic modulus was observed for dehydrated TADM than cornea ($P = 0.004$). After hydration, the tangent modulus at a stress of 100 KPa and elastic modulus of TADM were significantly decreased ($P = 0.021$ and $P < 0.001$, respectively).

Histology and Electron Microscopy of TADM

H&E staining demonstrated that the TADM consisted of dense collagen fibrils without a visible cellular component (Fig. 4A). As shown in Figure 4B, picrosirius red staining revealed that the TADM was composed mainly of type I collagen with some scattered type III collagen. As shown in Figure 4C, electron microscopy revealed that the collagen fibrils in the lamellae were organized. The mean collagen fibril diameter was 98.2 ± 19.1 nm, and the mean interfibrillar spacing was 99.8 ± 15.4 nm.

Ocular Signs and Graft Characteristics Following Lamellar Keratoplasty With TADM

No severe ocular complications were observed after lamellar keratoplasty. The graft was edematous, and the contour was visible at the time of transplantation and 1 week after surgery. The contour of the graft was invisible 1 month after
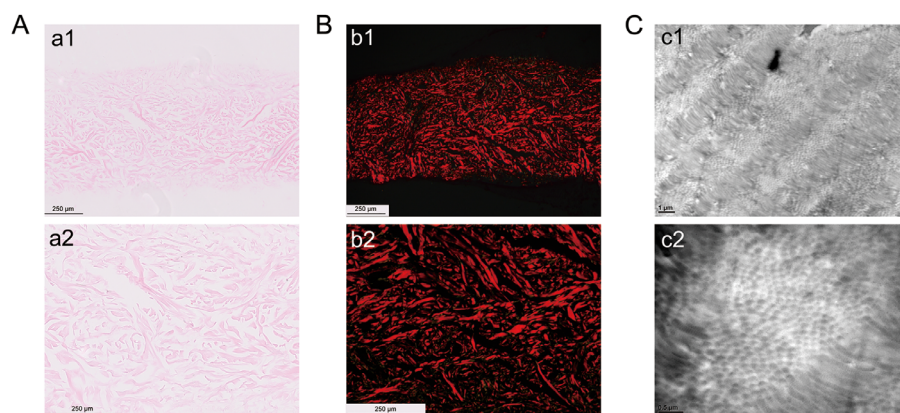
FIGURE 4. Histology and electron microscopy of TADM. H&E and picrosirius red staining and electron microscopy of TADM. **(A)** H&E staining of TADM at low *(a1)* and high *(a2)* magnification; **(B)** Picrosirius red staining of TADM at low *(b1)* and high *(b2)* magnification. **(C)** Electron microscopy of TADM at low *(c1)* and high *(c2)* magnification (representative of three independent experiments).

surgery, as shown in Figure 5A. The graft became clearer and more transparent on gross observation and, similar to the normal cornea, was completely transparent 6 months after surgery by slit-lamp microscopy. All of the grafts were covered with complete epithelium 1 month after surgery except for the grafts at the sutures shown in Figure 5B. Neovascularization was initially observed at 1 month in 87.5% of the grafts and had faded completely 6 months after surgery.

The thickness of the transplant area was significantly increased at 1 month, resulting from obvious graft edema, as shown by AS-OCT ($P = 0.025$). As the absorbance of the graft edema, the central corneal thickness decreased significantly at 6 months and was similar to the thickness of the normal cornea ($P = 0.48$), as shown in Figures 5C and 5D.

Transparency and Histology of Transplantation Area

The transmittance of the transplant area was significantly worse than that of the normal cornea at all wavelengths at 3 months. No significant differences in transmittance from 420–900 nm between the transplant area and normal cornea were found at 6 months, as shown in Figure 6A.

At 3 months after surgery, the graft was covered with completely stratified columnar epithelium, and keratocytes had repopulated the graft, as shown by H&E staining in Figure 6B,b1. The collagen arrangement in the graft was looser than that in the original cornea stroma, and the histological interface between the graft and original stroma was visible. The reconstructed graft was similar to the original stroma in terms of collagen organization, and the histological interface between the graft and original stroma was nearly invisible at 6 months, as shown in Figure 6B,b2. Additionally, the reconstructed graft was mainly composed of type I collagen at 3months, as shown in Figure 6C,c1. Figure 6C,c2 showed that the amount of type III collagen increased in the reconstructed graft at 6 months and had replaced the original graft. Completely differentiated epithelium covered the grafts at 3 and 6 months, as shown by the positive staining with cytokeratin 3/12 antibody in Figure 6D. A few grafts (1/8) were infiltrated with macrophages at 3 months, and no

macrophages were observed in the grafts at 6 months based on positive staining with CD68, as shown in Figure 6E.

DISCUSSION

In the present study, high-transmittance TADM was obtained, and after lamellar keratoplasty, the TADM demonstrated ideal optical, mechanical, and histological properties and satisfactory biocompatibility.

The dermis can be divided into two main sections with different collagen organizations, the upper papillary layer and the deeper reticular layer. The papillary layer contains dense, thin collagen fibrils less than 10 nm in diameter, while collagenous bundles in the reticular dermis are comparatively looser and greater than 50 nm in diameter.[13] ADM is a dermis-derived graft.[8] Thus, ADM obtained at different depths should have divergent histologic and transparent properties. Our previous research did not consider heterogeneity in the transparency of full-thickness ADM grafts. There are no standard reported methods for exploring the transparency distribution in soft tissue. Previous research on the microstructure of the corneal stroma has demonstrated that sucrose immersion followed by cryosectioning maintained the molecular bonds and protein secondary structures, as shown by infrared spectroscopy,[14] and that freezing had little effect on the fibril arrangement, as revealed by X-ray scattering.[15,16] Thus a stepwise sectioning strategy was applied to determine the transparency distribution in the ADM with increasing depth. The results in the present research demonstrated that the transparency increased as the depth increased. According to previous research, the transparency of the corneal stroma is mainly determined by the highly organized collagen fibril arrangement, specifically the collagen fibril diameter and interfibrillar spacing.[17] In the present research, H&E staining revealed more ordered collagenous bundles in the deeper ADM than in the superficial ADM, which was consistent with the transparency distribution results.

According to the transparency distribution, the deepest layer of the ADM was isolated as TADM. TADM had a transmittance curve similar to that of the normal cornea, including the same short-wavelength light-blocking function and high transmission for other wavelengths in the visible spectrum. The transparency of decellularized porcine corneal stroma
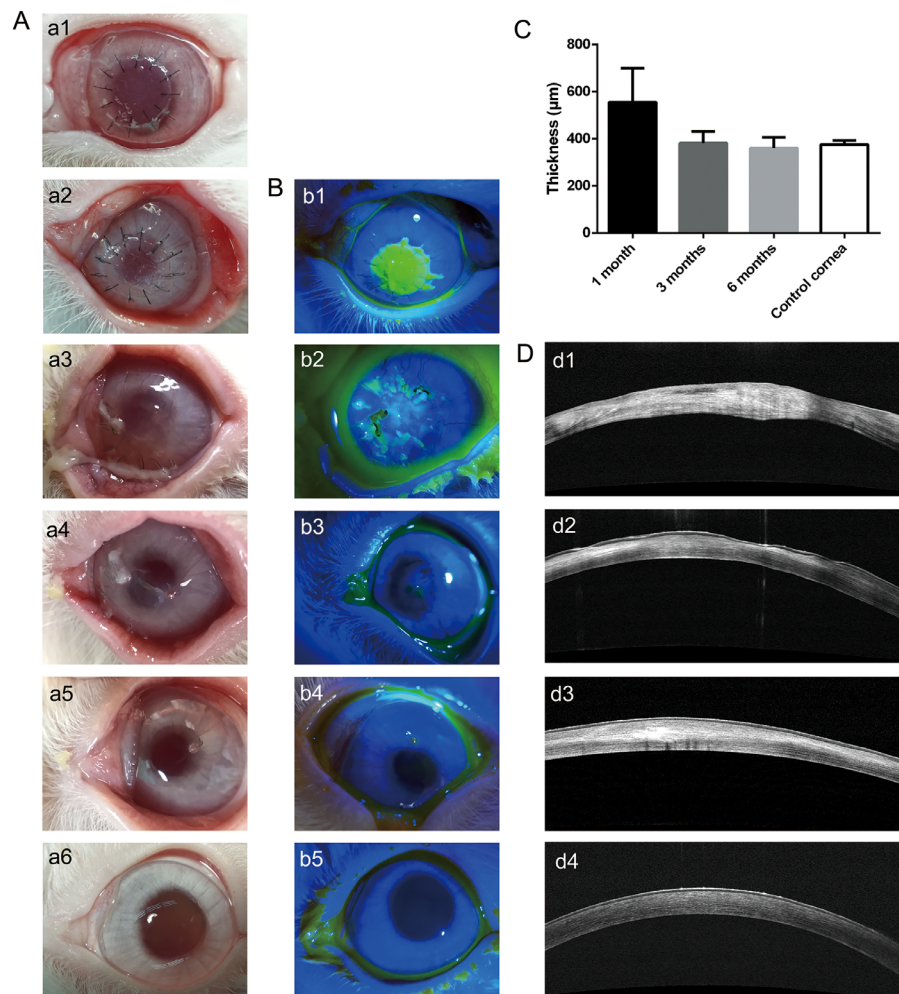
FIGURE 5. Characteristics of the cornea and graft after lamellar keratoplasty with TADM. Characteristics of the cornea and graft following lamellar keratoplasty evaluated by slit-lamp examination and AS-OCT at baseline and 1 week, 1 month, 3 months, and 6 months after surgery. **(A)** Anterior segment image by slit-lamp examination at the time of transplantation *(a1)*; 1 week *(a2)*, 1 month *(a3)*, 3 months *(a4)* and 6 months *(a5)* after surgery; and unoperated control cornea *(a6)* (representative of eight rabbits). **(B)** Corneal fluorescein staining 1 week *(b1)*, 1 month *(b2)*, 3 months *(b3)*, and 6 months *(b4)* after surgery and unoperated control cornea *(b5)* (representative of eight rabbits). **(C)** Central corneal thickness 1 month, 3 months, and 6 months after surgery obtained by AS-OCT compared with control cornea. **(D)** Postoperative AS-OCT images at 1 month *(d1)*, 3 months *(d2)*, and 6 months *(d3)* and unoperated control cornea *(d6)* (representative of eight rabbits).

is different among various studies. Several specified decellularization procedures, including methods based on gradient osmotic pressure and phospholipase, have been used to obtain acellular stroma with transparency similar to that of normal corneal.[18,19] In addition, cross-linked recombinant human collagen III but not collagen I revealed transparency similar to that of the cornea; however, the short-wavelength light-blocking feature was lacking, as reported in previous research.[20–23]

The mechanical properties of the cornea are crucial for maintaining the stability of its shape and curvature. The modulus of decellularized porcine corneal stroma has been reported to differ among different studies, and the disparity in decellularization processes may be one of the influencing factors.[24,25] Recombinant human collagen III with fabricated through collagen superimposition and cross-linking has an elastic modulus similar to that of cornea.[21,26] Actually, previous research on the mechanical properties of cornea substitutes has focused on only the elastic modulus and

tensile strength. Corneal tissue is viscoelastic and behaves according to an exponential stress-strain constitutive equation.[27] The present research demonstrates that the TADM and normal cornea have similar typical viscoelastic material stress-strain curves. The elastic modulus of the dehydrated TADM was higher than that of the normal cornea; however, dehydrated TADM had a lower tangent modulus under comparatively lower stress. The disparity in mechanical properties might be due to differences in the collagenous structure between the corneal stroma and dermis.

The corneal stroma is composed of highly organized collagen fibril-based lamellae with uniform fibril diameters and interfibrillar spacing that determine its transparency.[28] Decellularized porcine corneal stroma has nearly the same arrangement of collagen fibrils as normal human corneal stroma due to its origin.[29,30] Through advanced fabrication processes, recombinant human collagen grafts contain collagen fibrils with a consistent diameter and an ordered uniaxial arrangement slightly different from those of corneal
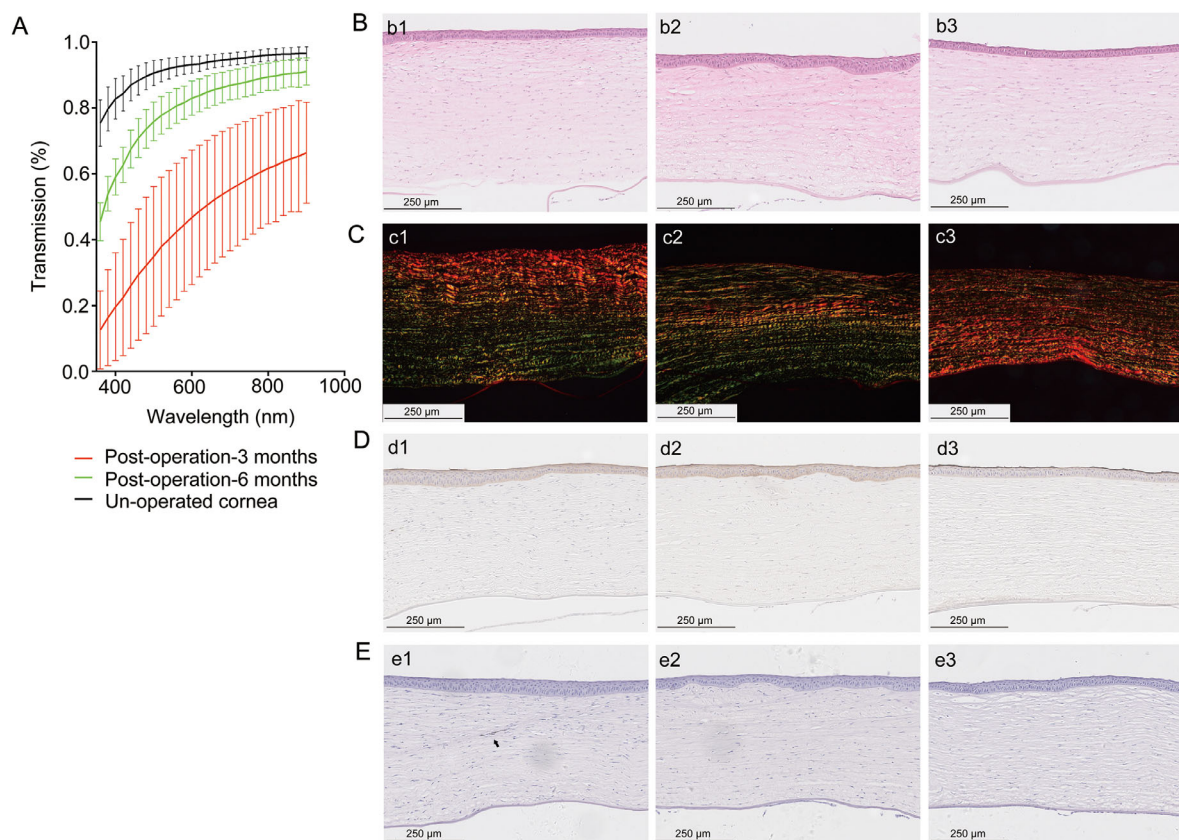
FIGURE 6. Transparency and histology of the transplant area. Transparency was evaluated by light transmittance, histology and collagen composition of the postoperative transplant area at 3 months and 6 months. **(A)** Light transmittance of the postoperative transplant area at 3 months and 6 months and unoperated cornea (n = 4, respectively). **(B)** H&E staining of the postoperative transplant area at 3 months *(b1)* and 6 months *(b2)* and unoperated cornea *(b3)*. **(C)** Picrosirius red staining of the postoperative transplant area at 3 months *(c1)* and 6 months *(c2)* and unoperated cornea *(c3)*. **(D)** Cytokeratin 3/12 staining of the postoperative transplant area at 3 months *(d1)* and 6 months *(d2)* and unoperated cornea *(d3)*. **(E)** CD68 staining of the postoperative transplant area at 3 months *(e1)* and 6 months *(e2)* and unoperated cornea *(e3)* (representative of four rabbits at 3 and 6 months, respectively).

stroma, which consists mainly of biaxially organized collagen lamellae.[21–23] The TADM in this study was derived from the reticular layer of dermis, which has much thicker collagen fibrils than the normal cornea.[4] H&E staining demonstrated that the TADM had a less organized dense collagen construction.

Acellular collagenous biomaterials can serve as stromal scaffolds to support epithelium and keratocyte growth and complete cornea reconstruction.[4,20,31] In the present study, complete re-epithelialization was observed for all grafts 1 month postoperatively. The rate of re-epithelization was similar to that of some other biomaterial scaffolds.[20,32,33] However, some studies have reported complete epithelial regeneration within a week after transplantation, especially for recombinant human collagen grafts.[19,22,26] Different decellularization processes can cause different forms of damage to the extracellular matrix and cell adhesion motif of the stroma, which may postpone re-epithelialization.[25] Additionally, variations in the collagen interfibrillar spacing causing different thicknesses after postoperative edema and distinct levels of smoothness resulting from different fabrication processes can also influence epithelial growth. The TADM showed keratocyte repopulation 3 months after surgery in this study. These results demonstrate that the TADM has ideal biocompatibility that supports keratocyte ingrowth for complete regeneration. Neovascularization was

observed in most of the grafts at 1 month and gradually faded over the follow-up period. Graft vascularization has also been observed for other collagenous scaffolds, and in most cases, the neovascularization receded after complete corneal reconstruction.[20,34,35] A certain degree of temporary reversible vascularity can promote corneal reconstruction and will not induce severe inflammation or rejection.

Collagen fibrils in the corneal stroma mainly consist of type I collagen. By contrast, type III collagen is barely present and will increase during wound healing and stromal remodeling as an intermediate collagen.[36,37] After keratoplasty, the levels of type III collagen and large proteoglycans in the regenerating area are increased and gradually decrease as the reconstruction process proceeds.[38] A previous study using recombinant human collagen III grafts for lamellar keratoplasty demonstrated that type III collagen is gradually replaced by type I collagen during remodeling.[39] In the present research, the grafts were mainly type I collagen, and the collagen fibrils were looser than the normal cornea stroma at 3 months. At 6 months postoperatively, a large amount of type I collagen had been replaced by type III collagen in the graft, and the organization of the reconstructed stroma was similar to that of the control cornea. The more organized collagen fibril might contribute to the more transparent postoperative cornea. The transformation in the collagen types and organization demonstrated the

remodeling processes of the repopulated keratocytes. Normally, most of the type III collagen is replaced by type I collagen during remodeling, which was not observed in this study, possibly because of the short follow-up time.

Currently, decellularized porcine corneal stroma and recombinant human collagen III are two major biomaterial stroma substitutes that have already been applied in clinical practice.[40–42] Decellularized porcine corneal stroma has ideal biocompatibility and nearly the same structure as human corneal stroma, but a drawback is its potential for transmitting animal pathogens. Recombinant human collagen III simulates the collagen organization of corneal stroma and has outstanding transparency.[21] The TADM in the present research is isolated from dermis and thus is naturally distinct from corneal stroma by histology. However, TADM has prominent advantages over other biomaterial scaffolds. The processes for fabricating TADM are easier. It is also abundantly available and does not raise ethical issues. Considering the graft size and thickness required for keratoplasty, the biomaterial might be derived from the patient's own dermis without much trauma.

The present research revealed the transparency distribution of ADM and a method for obtaining TADM and further demonstrated the ideal transparency and mechanical properties and satisfactory biocompatibility of TADM when applied in central lamellar keratoplasty. The research provided the potential for TADM application in lamellar keratoplasty in clinical practice to eliminate the issue of donor cornea shortages.

Acknowledgments

Disclosure: **Y. Wang**, None; **J. Ma**, None; **X. Jiang**, None; **Z. Liu**, None; **J. Yang**, None; **X. Li**, None

References

1. Whitcher JP, Srinivasan M, Upadhyay MP. Corneal blindness: a global perspective. *Bull World Health Organ*. 2001;79:214–221.
2. George AJ, Larkin DF. Corneal transplantation: the forgotten graft. *Am J Transplant*. 2004;4:678–685.
3. Gain P, Jullienne R, He Z, et al. Global Survey of Corneal Transplantation and Eye Banking. *JAMA Ophthalmol*. 2016;134:167–173.
4. Brunette I, Roberts CJ, Vidal F, et al. Alternatives to eye bank native tissue for corneal stromal replacement. *Prog Retin Eye Res*. 2017;59:97–130.
5. Kymionis GD, Mikropoulos DG, Portaliou DM, et al. New perspectives on lamellar keratoplasty. *Adv Ther*. 2014;31:494–511.
6. Matthyssen S, Van den Bogerd B, Dhubhghaill SN, Koppen C, Zakaria N. Corneal regeneration: A review of stromal replacements. *Acta Biomaterialia*. 2018;69:31–41.
7. Wilson SL, Sidney LE, Dunphy SE, Rose JB, Hopkinson A. Keeping an eye on decellularized corneas: a review of methods, characterization and applications. *J Funct Biomater*. 2013;4:114–161.
8. Daar DA, Gandy JR, Clark EG, Mowlds DS, Paydar KZ, Wirth GA. Plastic surgery and acellular dermal matrix: highlighting trends from 1999 to 2013. *World J Plast Surg*. 2016;5:97–108.
9. Liu Z, Ji J, Zhang J, et al. Corneal reinforcement using an acellular dermal matrix for an analysis of biocompatibility, mechanical properties, and transparency. *Acta Biomater*. 2012;8:3326–3332.
10. Jiang X, Wang Y, Qiu W, et al. Corneal stromal transplantation with human-derived acellular dermal matrix for pellucid marginal corneal degeneration: a nonrandomized clinical trial. *Transplantation*. 2019;103:e172–e179.
11. Coelho PGB, Souza MV, Conceicao LG, Viloria MIV, Bedoya SAO. Evaluation of dermal collagen stained with picrosirius red and examined under polarized light microscopy. *An Bras Dermatol*. 2018;93:415–418.
12. Chang SH, Mohammadvali A, Chen KJ, et al. The relationship between mechanical properties, ultrastructural changes, and intrafibrillar bond formation in corneal UVA/riboflavin cross-linking treatment for keratoconus. *J Refract Surg*. 2018;34:264–272.
13. Ventre M, Mollica F, Netti PA. The effect of composition and microstructure on the viscoelastic properties of dermis. *J Biomechan*. 2009;42:430–435.
14. Zhang L, Aksan A. Fourier transform infrared analysis of the thermal modification of human cornea tissue during conductive keratoplasty. *Appl Spectrosc*. 2010;64:23–29.
15. Boote C, Du Y, Morgan S, et al. Quantitative assessment of ultrastructure and light scatter in mouse corneal debridement wounds. *Invest Ophthalmol Visual Sci*. 2012;53:2786–2795.
16. Sheppard J, Hayes S, Boote C, Votruba M, Meek KM. Changes in corneal collagen architecture during mouse postnatal development. *Invest Ophthalmol Visual Sci*. 2010;51:2936–2942.
17. Meek KM, Knupp C. Corneal structure and transparency. *Progr Retinal Eye Res*. 2015;49:1–16.
18. Lin Y, Zheng Q, Hua S, Meng Y, Chen W, Wang Y. Cross-linked decellularized porcine corneal graft for treating fungal keratitis. *Sci Rep*. 2017;7:9955.
19. Wu Z, Zhou Y, Li N, et al. The use of phospholipase A(2) to prepare acellular porcine corneal stroma as a tissue engineering scaffold. *Biomaterials*. 2009;30:3513–3522.
20. Rafat M, Li F, Fagerholm P, et al. PEG-stabilized carbodiimide crosslinked collagen-chitosan hydrogels for corneal tissue engineering. *Biomaterials*. 2008;29:3960–3972.
21. Liu W, Merrett K, Griffith M, et al. Recombinant human collagen for tissue engineered corneal substitutes. *Biomaterials*. 2008;29:1147–1158.
22. Liu W, Deng C, McLaughlin CR, et al. Collagen-phosphorylcholine interpenetrating network hydrogels as corneal substitutes. *Biomaterials*. 2009;30:1551–1559.
23. Hayes S, Lewis P, Islam MM, et al. The structural and optical properties of type III human collagen biosynthetic corneal substitutes. *Acta Biomater*. 2015;25:121–130.
24. Shao Y, Tang J, Zhou Y, et al. A novel method in preparation of acellularporcine corneal stroma tissue for lamellar keratoplasty. *Am J Transl Res*. 2015;7:2612–2629.
25. Hashimoto Y, Funamoto S, Sasaki S, et al. Preparation and characterization of decellularized cornea using high-hydrostatic pressurization for corneal tissue engineering. *Biomaterials*. 2010;31:3941–3948.
26. Merrett K, Fagerholm P, McLaughlin CR, et al. Tissue-engineered recombinant human collagen-based corneal substitutes for implantation: performance of type I versus type III collagen. *Invest Ophthalmol Vis Sci*. 2008;49:3887–3894.
27. Hoeltzel DA, Altman P, Buzard K, Choe K. Strip extensiometry for comparison of the mechanical response of bovine, rabbit, and human corneas. *J Biomech Eng*. 1992;114:202–215.
28. Hassell JR, Birk DE. The molecular basis of corneal transparency. *Exp Eye Res*. 2010;91:326–335.

29. Fu Y, Fan X, Chen P, Shao C, Lu W. Reconstruction of a tissue-engineered cornea with porcine corneal acellular matrix as the scaffold. *Cells Tissues Organs*. 2010;191:193–202.

30. Hashimoto Y, Hattori S, Sasaki S, et al. Ultrastructural analysis of the decellularized cornea after interlamellar keratoplasty and microkeratome-assisted anterior lamellar keratoplasty in a rabbit model. *Sci Rep*. 2016;6:27734.

31. Uzunalli G, Soran Z, Erkal TS, et al. Bioactive self-assembled peptide nanofibers for corneal stroma regeneration. *Acta Biomat*. 2014;10:1156–1166.

32. Zhang C, Nie X, Hu D, et al. Survival and integration of tissue-engineered corneal stroma in a model of corneal ulcer. *Cell Tissue Res*. 2007;329:249–257.

33. Hashimoto Y, Funamoto S, Sasaki S, et al. Corneal regeneration by deep anterior lamellar keratoplasty (DALK) using decellularized corneal matrix. *PloS One*. 2015;10: e0131989.

34. Lin XC, Hui YN, Wang YS, Meng H, Zhang YJ, Jin Y. Lamellar keratoplasty with a graft of lyophilized acellular porcine corneal stroma in the rabbit. *Vet Ophthalmol*. 2008;11:61–66.

35. van Essen TH, van Zijl L, Possemiers T, et al. Biocompatibility of a fish scale-derived artificial cornea: Cytotoxicity, cellular adhesion and phenotype, and in vivo immunogenicity. *Biomaterials*. 2016;81:36–45.

36. Robert L, Legeais JM, Robert AM, Renard G. Corneal collagens. *Pathol Biol (Paris)*. 2001;49:353–363.

37. Li Y, Chen HJ, Zhang H, Wu JG, Hu YT, Ma ZZ. Effects of different sutures on fibrosis and wound healing in a rabbit model of corneal wounds. *Exp Therap Med*. 2016;12:2827–2834.

38. Kato T, Nakayasu K, Kanai A. Corneal wound healing: immunohistological features of extracellular matrix following penetrating keratoplasty in rabbits. *Jpn J Ophthalmol*. 2000;44:334–341.

39. Ljunggren MK, Elizondo RA, Edin J, et al. Effect of surgical technique on corneal implant performance. *Transl Vis Sci Technol*. 2014;3:6.

40. Zhang MC, Liu X, Jin Y, Jiang DL, Wei XS, Xie HT. Lamellar keratoplasty treatment of fungal corneal ulcers with acellular porcine corneal stroma. *Am J Transplant*. 2015;15:1068–1075.

41. Fagerholm P, Lagali NS, Merrett K, et al. A biosynthetic alternative to human donor tissue for inducing corneal regeneration: 24-month follow-up of a phase 1 clinical study. *Sci Transl Med*. 2010;2:46ra61.

42. Buznyk O, Pasyechnikova N, Islam MM, Iakymenko S, Fagerholm P, Griffith M. Bioengineered corneas grafted as alternatives to human donor corneas in three high-risk patients. *Clin Transl Sci*. 2015;8:558–562.